PHYSICAL REVIEW C, VOLUME 60, 011303

Differential quadrupole moment measurements of the $1/2^+[660]$ ($i_{13/2}$) neutron intruder band in ^{133}Nd and ^{135}Nd

F. G. Kondev,* M. A. Riley, D. J. Hartley,† T. B. Brown,‡ R. W. Laird, M. Lively, J. Pfohl, and R. K. Sheline
Department of Physics, Florida State University, Tallahassee, Florida 32306

E. S. Paul, D. T. Joss,§ P. J. Nolan, and S. L. Shepherd
Oliver Lodge Laboratory, University of Liverpool, Liverpool L69 7ZE, United Kingdom

R. M. Clark and P. Fallon
Nuclear Science Division, Lawrence Berkeley National Laboratory, Berkeley, California 94720

D. G. Sarantites, M. Devlin, D. R. LaFosse,‖ and F. Lerma
Department of Chemistry, Washington University, St. Louis, Missouri 63130

R. Wadsworth, I. M. Hibbert,¶ and N. J. O'Brien
Department of Physics, University of York, York Y01 5DD, United Kingdom

J. Simpson
CLRC, Daresbury Laboratory, Daresbury, Warrington WA4 4AD, United Kingdom

D. E Archer
Lawrence Livermore National Laboratory, Livermore, California 94550

(Received 28 December 1998; published 16 June 1999)

Quadrupole moment measurements of the $1/2^+[660]$ ($i_{13/2}$) bands in ^{133}Nd ($N=73$) and ^{135}Nd ($N=75$) were performed using the Doppler-shift attenuation method. These results, coupled with the previously measured Q_0 for the same configuration in ^{137}Nd ($N=77$), clearly demonstrate a trend of decreasing quadrupole deformation with increasing neutron number. The larger quadrupole moment in ^{133}Nd compared with that in ^{135}Nd and ^{137}Nd offers evidence for the role played by the large shell gap at $N=72$ for $\beta_2 \sim 0.35-0.40$ in stabilizing the shape at enhanced deformation. The comparison of results from gating below and above the level of interest provides information on the time scale of the sidefeeding contributions to highly deformed structures in the $A\sim 130$ region. [S0556-2813(99)50507-4]

PACS number(s): 21.10.Tg, 21.10.Re, 23.20.Lv, 27.60.+j

The occupation of the $i_{13/2}$ neutron intruder orbitals is known to be a prominent factor in driving the nuclear shape towards higher deformation for nuclei in the $A\sim 130$ region [1]. In addition, the accumulated wealth of new experimental data reveals that the role played by the large shell gaps at $N=72$ and $Z=58$ ($\beta_2 \sim 0.35-0.40$) may also be as important as the occupation of the $\nu i_{13/2}$ intruder orbital (see for example Ref. [2] and references therein). The odd-N Nd ($Z=60$) isotopes offer an excellent opportunity to elucidate the interplay between these two underlying mechanisms (shell gaps versus intruder occupation) which are common to all superdeformed regions. Collective structures built upon the $\nu 1/2^+[660]$ ($i_{13/2}$) orbital have been observed in the chain of odd-N Nd isotopes from ^{133}Nd up to ^{137}Nd [3,4]. These bands have been connected to the normally deformed structures [4–9], so that their spin, parity, and excitation energy are unambiguously determined. In addition, the g-factor experiment performed in the case of ^{133}Nd [10] independently confirms the $\nu 1/2^+[660]$ configuration assignment.

Information regarding the importance of the occupation of specific orbitals along with the ''core stabilization'' effect from deformed shell gaps comes from accurate lifetime measurements. While the quadrupole moment Q_0, for the $\nu i_{13/2}$ highly deformed, sometimes called ''superdeformed,'' bands in ^{133}Nd, ^{135}Nd, and ^{137}Nd has been measured in the past using both the centroid-shift and line shape Doppler-shift attenuation (DSAM) techniques [10–14], conclusive comparisons were limited owing to systematic distinctions between experimental setups such as varying reactions and target retardation properties. One of the main problems results from the differences in the parametrization of the nuclear and electronic stopping powers, which act as an ''internal clock''

*Present address: Physics Division, Argonne National Laboratory, Argonne, Illinois 60439.

†Present address: Department of Physics and Astronomy, University of Tennessee, Knoxville, Tennessee 37996.

‡Present address: Department of Physics and Astronomy, University of Kentucky, Lexington, Kentucky 40506.

§Present address: School of Sciences, Staffordshire University, Stoke-on-Trent ST4 2DE, United Kingdom.

‖Present address: Department of Physics and Astronomy, State University of New York at Stony Brook, New York 11794.

¶Present address: Oliver Lodge Laboratory, University of Liverpool, Liverpool L69 7ZE, United Kingdom.

in the DSAM lifetime measurements. This leads to large variations in the measured Q_0 values being reported for the same band by different authors. The results from the recoil-distance method measurements for the bands in ^{133}Nd [15] and ^{135}Nd [16], which are free from the pitfalls introduced by the parametrizations of the stopping powers, have other setbacks that do not enable definitive comparisons of the quadrupole deformations. For example, they are limited only to a few low-spin in-band levels and have large errors. The absence of adequate experimental information on the time structure of the sidefeeding contributions also results in an additional inaccuracy in the measured quadrupole moments. In the current work we have greatly reduced these problems by measuring the lifetime decay properties of these bands under similar experimental conditions in terms of angular momentum input, excitation energy, and recoil velocity profile. The former conditions were verified by an off-line multiplicity (k) and total energy (H) analysis, see below and Ref. [17], and the latter from an earlier thin target dataset using the same reaction. By exploiting the high efficiency and resolving power of the modern γ-ray detector arrays it was possible to greatly minimize the effect of sidefeeding on the measured quadrupole deformations, by gating on Doppler-shifted transitions at the top of the band of interest, thus gaining insight into the nature and time scale of the sidefeeding to the highly deformed bands.

High-spin states in ^{133}Nd and ^{135}Nd were populated in the $(1p1\alpha2n)$ and $(3p2n)$ channels of the ^{35}Cl+^{105}Pd reaction, respectively, at a beam energy of 173 MeV. The target consisted of a 1 mg/cm^2 thick ^{105}Pd foil mounted on a 17 mg/cm^2 Au backing which stops the recoiling nuclei. The beam was provided by the 88-Inch Cyclotron at the Lawrence Berkeley National Laboratory. Emitted γ rays were detected using the GAMMASPHERE spectrometer [18] consisting for this experiment of 97 HPGe detectors. The evaporated charged particles were identified with the MICROBALL detector array [19] which allowed a clean separation of the different charged particle channels. A total of 1.9×10^8 and 8.4×10^7 three-fold or higher Compton suppressed coincidence events were collected in the $1p1\alpha$ and $3p$ particle gated channels, respectively.

The quadrupole deformations were extracted using the centroid-shift DSAM technique [20] in two different ways. In the first method, the data were sorted into two-dimensional matrices in which one axis consisted of ''forward'' ($\theta=31.7°$ and 37.4°) or ''backward'' (142.6° and 148.3°) detectors and the other axis was any coincident detector. Spectra were generated by summing gates on the cleanest, fully stopped transitions at the bottom of the band of interest and projecting the events onto the ''forward'' and ''backward'' axes. These spectra were then used to extract the fraction of the full Doppler shift $F(\tau)$, which represents the ratio of the average recoil velocity at which a state decays to the average initial recoil velocity, for transitions within the band of interest. The sidefeeding contributions are fully in effect when the Q_0 values are deduced using this approach, since the measured $F(\tau)$ values depend not only on the lifetime of a particular state, but also on the time history of all levels within the cascades that precede it. In the second method, the data were sorted into a number of spectra for events detected at ''forward,'' 90°, and ''backward'' angles by using single and double gates on in-band ''moving'' transitions in any ring of detectors. Since the gating transitions are Doppler-shifted, ring-by-ring energy-dependent corrections were applied in the sorting procedure using the formula

$$C=C_0(1+F(\tau)\beta_0\cos\theta), \tag{1}$$

where C_0 and C are the raw and Doppler-adjusted channel numbers, respectively, and β_0 refers to the initial velocity of the recoiling nuclei, assuming that they are produced in the middle of the target. The $F(\tau)$ values for transitions within the band of interest were calculated (see below) iteratively by varying the in-band Q_0 until the Doppler-shifted peak centroids were perfectly matched in all detector rings. This allowed the correct coincidence relationships to be achieved in the gating procedure. Consequently, non-Doppler corrected spectra were written on disks and were used to extract the final $F(\tau)$ values. The implementation of this method made it possible to eliminate the effect of sidefeeding for states below those depopulated by the gating transitions. Examples of resulting background subtracted spectra for the bands in ^{133}Nd and ^{135}Nd are shown in Fig. 1 and Fig. 2, respectively. It should be noted that an additional monitoring of the sum energy and the multiplicity of the events (H–k plots) [17] were also performed in the off-line analysis procedure, which enabled us to track the properties of the entry point distributions within a given band.

In order to extract the intrinsic quadrupole moments from the experimental $F(\tau)$ values, calculations using the code FITFTAU [21] were performed. The $F(\tau)$ curves were generated under the assumption that the band has a constant Q_0 value. In the modeling of the slowing down process of the recoiling nuclei, the stopping powers were calculated using the 1995 version of the code TRIM [22] which uses the most recent evaluation of existing data. The corrections for multiple scattering were introduced using the prescription given

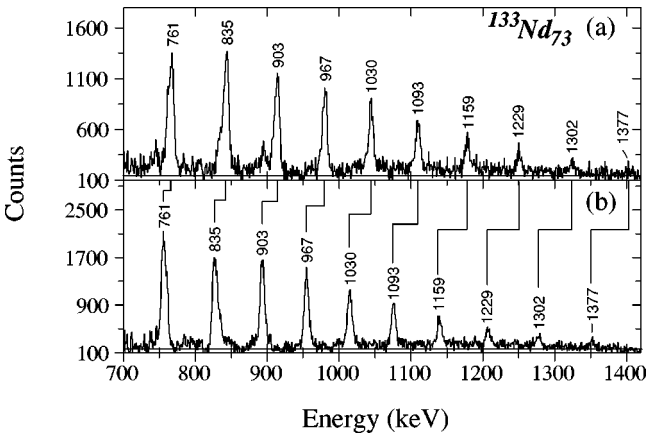

FIG. 1. Coincidence γ-ray spectra in the ''forward'' (a) and ''backward'' (b) group of detectors for the highly deformed $\nu1/2^+[660]$ ($i_{13/2}$) band in ^{133}Nd produced by combining all double gates on in-band transitions from 344.4 keV up to 1228.8 keV. The peaks are labeled with the unshifted γ-ray energies.

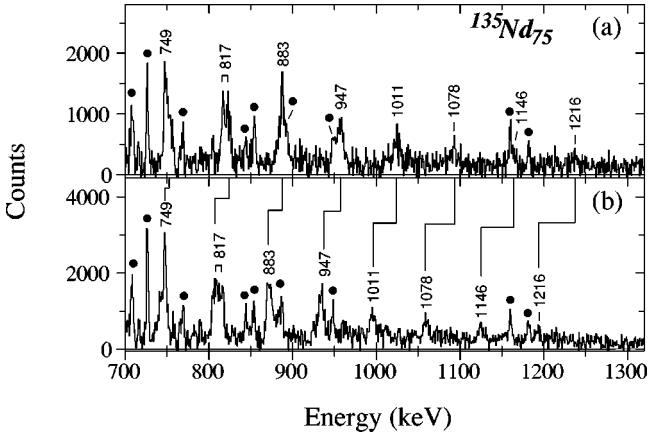

FIG. 2. Coincidence γ-ray spectra in the ''forward'' (a) and ''backward'' (b) group of detectors for the highly deformed $\nu 1/2^+[660]$ $(i_{13/2})$ band in ^{135}Nd produced by combining singles gates on 545.9, 676.5, 748.6, and 816.8 keV in-band transitions. The peaks are labeled with the unshifted γ-ray energies. The peaks labeled with filled circles correspond to stopped transitions below the $I^\pi = 25/2^+$ in-band level [4,7].

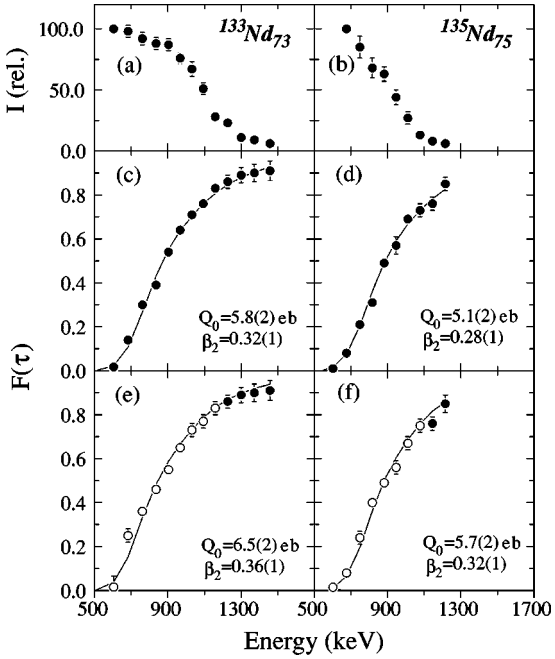

FIG. 3. Intensity profiles (a) and (b), $F(\tau)$ values, and corresponding quadrupole deformations deduced by gating on stopped transitions, depopulating low-spin in-band levels (c) and (d), and Doppler-shifted transitions depopulating high-spin in-band levels (e) and (f) for the highly deformed $\nu 1/2^+[660]$ $(i_{13/2})$ bands in ^{133}Nd and ^{135}Nd, respectively. The error bars reflect only the uncertainty in determining the peak centroids. The open symbols in panels (e) and (f) correspond to values deduced by gating above the level of interest. The solid lines represent best fit values.

by Blaugrund [23]. Where appropriate, the sidefeeding into each state was taken into account according to the experimental in-band intensity profile using a rotational cascade of three transitions having the same moment of inertia and quadrupole moment, Q_{0sf}, as the main band. It is important to note that the errors quoted in the current work reflect only the statistical uncertainties in the measurements of the γ-ray peak centroids. An additional 15–20 % systematic uncertainty, coming mainly from the knowledge of the stopping powers, should be included when comparisons with theoretical calculations or other Q_0 measurements are being made. The impact of the number of sidefeeding cascades on Q_0 was also investigated and found to be much smaller than the statistical uncertainties.

The $F(\tau)$ values and the corresponding precise quadrupole deformations deduced in the current work when gates were set on the stopped 408.2, 440.0, 513.1, and 603.2 keV transitions in ^{133}Nd, and the stopped 545.9 and 676.5 keV transitions in ^{135}Nd are shown in Figs. 3(c) and 3(d). Our observations are in agreement with the previously measured, but less precise, quadrupole deformations for the band in ^{133}Nd [11], as well as with the centroid-shift results for the structure in ^{135}Nd reported by Diamond *et al.* [12]. They clearly indicate that the band in ^{133}Nd is more deformed than that in ^{135}Nd. The comparison of the intensity profiles for these two bands, shown in Figs. 3(a) and 3(b), reveals that the sequence in ^{135}Nd has more sidefeeding intensity over a range of transitions for which the $F(\tau)$ values change very rapidly. Such behavior has led to speculations that the sidefeeding lifetimes could be much slower when compared with that for the in-band levels. In fact, the line shape analysis of ^{135}Nd in Ref. [12], as well as recent centroid-shift results of Ref. [13], suggested that the sidefeeding lifetimes were about a factor of four slower, thus leading to a deduced quadrupole deformation that exceeded the value in ^{133}Nd (see Table I). Figures 3(e) and 3(f) show our observations when spectra gated on Doppler-shifted transitions above the level of interest were used. We found roughly a 10% increase in the deformation of both these two bands, compared with values deduced when gates were set on stopped transitions, at the bottom of the bands. This corresponds to sidefeeding lifetimes only about 1.3–1.4 times slower than those for the in-band levels. Similar results for the ratio of in-band to sidefeeding lifetimes were recently reported by Clark *et al.* [24] in studying the relative deformations of structures that include one or two $i_{13/2}$ neutron orbitals in the neighboring ^{131}Ce and ^{132}Ce isotopes.

Table I summarizes the measured Q_0 values and the corresponding quadrupole deformations β_2, computed using the rotational ellipsoid formula of Ref. [25]. For comparison, previously measured values, as well as those for the same configuration in the neighboring ^{137}Nd and ^{131}Ce isotopes, which were populated with cross sections too low for reliable lifetime information to be obtained from our experiment, are also shown.

The present results, together with the significantly lower Q_0 value for the band in ^{137}Nd [11], clearly indicate a systematic decrease with N in the deformation of the $\nu 1/2^+[660]$ $(i_{13/2})$ bands. This experimental trend is now in agreement with predictions given in Refs. [7,11,26] using several theoretical approaches and general expectations. For example, Fig. 4(a) shows a comparison of the experimentally observed excitation energies as a function of spin for these

TABLE I. Quadrupole moments and deformations for the $\nu 1/2^+[660]$ bands in odd-N Ce and Nd nuclei.

Nucleus	Q_0, e b $[\beta_2]$ [a]		
	Present [b]	Previous	Reference
$^{131}Ce_{73}$		6.7(3) [0.39(1)]	[24]
		7.4(3) [0.43(1)] [c]	[24]
$^{133}Nd_{73}$	5.8(2) [0.32(1)]	6.0(7) [0.33(3)]	[11]
	6.5(2) [0.36(1)] [c]	6.7(7)[0.37(4)] [d]	[11]
		7.4(7)[0.41(3)] [e]	[10]
		6.7(11)[0.37(6)] [f]	[15]
$^{135}Nd_{75}$	5.1(2) [0.28(1)]	5.4(10) [0.30(5)]	[12]
	5.7(2) [0.32(1)] [c]	7.4(10) [0.40(5)] [g]	[12]
		7.3(10) [0.37(5)] [h]	[13]
		$7.2(^{+12}_{-15})[0.39(^{+7}_{-8})]$ [i]	[16]
$^{137}Nd_{77}$		4.0(5) [0.22(3)]	[11]

[a]Deduced using the centroid-shift technique with $Q_{0sf}=Q_0$.
[b]The uncertainties in the stopping powers may contribute an additional systematic error of 10–15 % in the absolute Q_0 values [24].
[c]Deduced by gating above the level of interest (see the text for details).
[d]Deduced using the line shape technique with $Q_{0sf}=5.3$ e b.
[e]Deduced using the line shape technique with sidefeeding time distributions about 1.4 times slower than the in-band lifetimes.
[f]Deduced using the recoil-distance technique from the partial lifetime of the 440.0 keV, $25/2^+\rightarrow 21/2^+$ in-band transition.
[g]Deduced using the line shape technique with $Q_{0sf}=3.5$ e b.
[h]Deduced using the centroid-shift technique with $Q_{0sf}=3.0\,(5)e$ b. Note that although the Q_0 value is nearly identical to that reported in Ref. [12] the quoted β_2 value is $\sim 7\%$ smaller.
[i]Deduced using the recoil-distance technique from the partial lifetime of the 676.5 keV, $37/2^+\rightarrow 35/2^+$ in-band transition.

sequences. It can be seen that they follow nearly in parallel as spin increases and importantly, that the structure in ^{133}Nd is lower in energy compared to those in ^{135}Nd ($\Delta E\sim 0.6$ MeV) and ^{137}Nd ($\Delta E\sim 1.6$ MeV). Bearing in mind the rapid downslope of the $1/2^+[660]$ ($i_{13/2}$) neutron orbital with increasing deformation, the higher excitation energy for the bands in ^{135}Nd and ^{137}Nd would indicate that they are less deformed, as illustrated in Fig. 4(b). Since at $N=73$ and $\beta_2\approx 0.35$ the neutron Fermi level resides at the boundary of the $N=72$ shell gap, the observed enhanced deformation in ^{133}Nd would offer good evidence for the particularly important role played by the latter in defining the equilibrium deformation.

Another interesting feature is the extra deformation observed for the $\nu 1/2^+[660]$ ($i_{13/2}$) band in ^{131}Ce ($Z=58$) [24] compared to the value in the ^{133}Nd ($Z=60$) $N=73$ isotone, see Table I. This comparison is reasonable since the quadrupole moment for the former band has been deduced in a manner similar to that for ^{133}Nd reported in the current work. Recent calculations based on the configuration-dependent cranked Nilsson-Strutinsky formalism [26] suggest that the presence of two proton ''holes'' in the upsloping $9/2^+[404]$ ($g_{9/2}$) proton orbital, combined with the large $Z=58$ shell gap at $\beta_2\sim 0.35$–0.40, provides a mechanism for the enhanced deformation in Ce compared to Nd nuclei. In a simplified way, the difference in deformation between the $N=73$ isotones

$$\delta\beta_2=\beta_2(^{131}\mathrm{Ce})-\beta_2(^{133}\mathrm{Nd})=0.43(1)-0.36(1)=0.07(2) \tag{2}$$

demonstrates that this effect is as large as $\sim 15\%$. Hence, by taking the measured quadrupole moment for the $\nu 1/2^+[660]$ ($i_{13/2}$) bands in ^{135}Nd and ^{137}Nd as a base, then one may expect $Q_0\sim 6.8(3)$ and 5.1(9) e b for the same configuration in the neighboring ^{133}Ce and ^{135}Ce nuclei, respectively. It should be kept in mind that recent lifetime measurements for higher seniority bands in ^{133}Ce [29], whose configurations are suggested to involve the $1/2^-$ [530] ($f_{7/2},h_{9/2}$) neutron coupled to the ^{132}Ce superdeformed core ($\pi 5^4\otimes\nu 6^2$) [30], yield $Q_0=7.4(7)$ and 7.5(8) e b.

In summary, precise differential quadrupole moment measurements were performed for the $\nu 1/2^+[660]$ ($i_{13/2}$) highly deformed bands in ^{133}Nd and ^{135}Nd. By exploiting the high efficiency and resolving power of the GAMMASPHERE spectrometer it was possible to greatly minimize the effect of unknown sidefeeding time contributions on the deduced quadrupole deformations. The new results obtained, together with data on ^{137}Nd, clearly establish a trend of decreasing deformation for the $\nu 1/2^+[660]$ ($i_{13/2}$) band as the neutron number increases, thus offering evidence about the important role played by the $N=72$ shell gap in ''stabilizing'' the nuclear shape at large deformation. The effect of the complementary $Z=58$ shell gap near $\beta_2\sim 0.35$–0.40, along with the

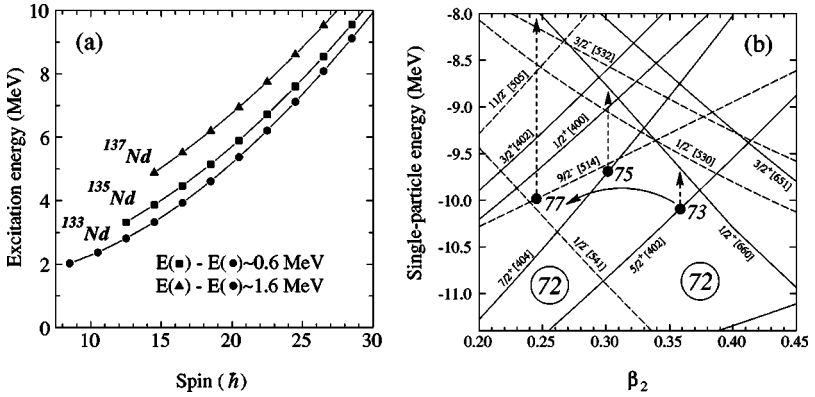

FIG. 4. (a) Excitation energies as a function of spin for the $\nu 1/2^+[660]$ ($i_{13/2}$) bands in ^{133}Nd [5,6], ^{135}Nd [4,7] and ^{137}Nd [8,9]. (b) Neutron single-particle levels as a function of quadrupole deformation ($\gamma=0°$, $\beta_4=0.0$) calculated using the Woods-Saxon potential [27] with parameters given by Nazarewicz *et al.* [28].

occupation probability of the $9/2^+[404]$ ($g_{9/2}$) proton orbital in Ce and Nd nuclei on the relative deformations of the $N=73$ isotones, has also been discussed.

The authors wish to extend their thanks to the staff of the LBNL GAMMASPHERE facility and the crew of the 88-Inch Cyclotron for their assistance during the experiment. The software support of D.C. Radford and H.Q. Jin is greatly appreciated. We are grateful to R. Darlington for help with the targets. Support for this work was provided by the U.S. Department of Energy under Contract No. DE-AC03-765F00098 and Grant No. DE-FG02-88ER40406, the National Science Foundation, the State of Florida, and the U.K. Engineering and Physical Sciences Research Council. M.A.R. and J.S. acknowledge financial support from a NATO. Discussions with Professor R.V.F. Janssens are gratefully acknowledged.

[1] R. Wyss, J. Nyberg, A. Johnson, R. Bengtsson, and W. Nazarewicz, Phys. Lett. B **215**, 211 (1988).
[2] A. Galindo-Uribarri, D. Ward, H.R. Andrews, G.C. Ball, D.C. Radford, V.P. Janzen, S.M. Mullins, J.C. Waddington, A.V. Afanasjev, and I. Ragnarsson, Phys. Rev. C **54**, 1057 (1996).
[3] R. Wadsworth *et al.*, J. Phys. G **13**, L207 (1987).
[4] E.M. Beck, F.S. Stephens, J.C. Bacelar, M.A. Deleplanque, R.M. Diamond, J.E. Draper, C. Duyar, and R.J. McDonald, Phys. Rev. Lett. **58**, 2182 (1987).
[5] D. Bazzacco *et al.*, Phys. Lett. B **309**, 235 (1993).
[6] D. Bazzacco *et al.*, Phys. Rev. C **49**, R2281 (1994).
[7] M.A. Deleplanque *et al.*, Phys. Rev. C **52**, R2302 (1995).
[8] S. Lunardi, R. Venturelli, D. Bazzacco, C.M. Petrache, C. Rossi-Alvarez, G. de Angelis, G. Vedovato, D. Bucurescu, and C. Ur, Phys. Rev. C **52**, R6 (1995).
[9] C.M. Petrache *et al.*, Nucl. Phys. **A617**, 228 (1997).
[10] N.H. Medina *et al.*, Nucl. Phys. **A589**, 106 (1995).
[11] S.M. Mullins, I. Jenkins, Y.-J. He, A.J. Kirwan, P.J. Nolan, J.R. Hughes, R. Wadsworth, and R. Wyss, Phys. Rev. C **45**, 2683 (1992).
[12] R.M. Diamond, C.W. Beausang, A.O. Macchiavelli, J.C. Bacelar, J. Brude, M.A. Deleplanque, J.E. Draper, C. Duyar, R.J. McDonald, and F.S. Stephens, Phys. Rev. C **41**, R1327 (1990).
[13] C.M. Petrache *et al.*, Phys. Rev. C **57**, R10 (1998).
[14] C.M. Petrache *et al.*, Phys. Lett. B **219**, 145 (1996).
[15] S.A. Forbes, G. Böhm, R.M. Clark, A. Dewald, R. Krücken, S.M. Mullins, P.J. Nolan, P.H. Regan, and R. Wadsworth, Z. Phys. A **352**, 15 (1995).
[16] P. Willsau *et al.*, Phys. Rev. C **48**, R494 (1993).
[17] M. Devlin, L.G. Sobotka, D.G. Sarantites, and D.R. LaFosse, Nucl. Instrum. Methods Phys. Res. A **383**, 506 (1996).
[18] R. Janssens and F. Stephens, Nucl. Phys. News **6**, 9 (1996).
[19] D.G. Sarantites, P.-F. Hua, M. Devlin, L.G. Sobotka, J. Elson, J.T. Hood, D.R. LaFosse, J.E. Sarantites, and M.R. Maier, Nucl. Instrum. Methods Phys. Res. A **381**, 418 (1996).
[20] T.K. Alexander and J.S. Forster, *Advances in Nuclear Physics* (Plenum, New York, 1978), Vol. 10, p. 197.
[21] E.F. Moore *et al.*, Phys. Rev. C **55**, R2150 (1997).
[22] J.F. Ziegler, J.P. Biersack, and U. Littmark, *The Stopping and Range of Ions in Solids* (Pergamon, New York, 1985); J.F. Ziegler (private communication).
[23] A.E. Blaugrund, Nucl. Phys. **88**, 501 (1966).
[24] R.M. Clark *et al.*, Phys. Rev. Lett. **76**, 3510 (1996).
[25] K.E.G. Löbner, M. Vetter, and V. Hönig, Nucl. Data, Sect. A **7**, 495 (1970).
[26] A.V. Afanasjev and I. Ragnarsson, Nucl. Phys. **A608**, 176 (1996).
[27] S. Cwiok, J. Dudek, W. Nazarewicz, J. Skalski, and T. Werner, Comput. Phys. Commun. **46**, 379 (1987).
[28] W. Nazarewicz, M.A. Riley, and J.D. Garrett, Nucl. Phys. **A512**, 61 (1990).
[29] K. Hauschild *et al.*, Phys. Rev. C **52**, R2281 (1995).
[30] K. Hauschild *et al.*, Phys. Lett. B **353**, 438 (1995).